Available online at www.sciencedirect.com
SCIENCE DIRECT®
European Journal of Pharmacology 478 (2003) 161–171
www.elsevier.com/locate/ejphar

Use-dependent blockade of cardiac pacemaker current (I_f) by cilobradine and zatebradine

Pierre Paul Van Bogaert*, François Pittoors

Laboratory for Electrophysiology, Department of Physiology, University of Antwerp (RUCA), Groenenborgerlaan 171, B-2020 Antwerp, Belgium

Received 24 March 2003; received in revised form 27 August 2003; accepted 29 August 2003

Abstract

The action of the bradycardiac agents, cilobradine (DK-AH269) and zatebradine (UL-FS49), on the cardiac pacemaker current (I_f) was investigated on short Purkinje fibres from sheep hearts, using the two-microelectrode voltage-clamp technique, and on isolated rabbit sino-atrial cells with the patch clamp technique. These drugs reduce dose dependently the amplitude of the I_f, without modifying either the voltage dependence or the kinetics of channel activation. When voltage-clamp pulse trains were applied, cilobradine induced a use-dependent blockade of I_f that was stronger and faster than that with zatebradine. Recovery from blockade during prolonged hyperpolarization was significantly faster with zatebradine. Presumably, both drugs block the hyperpolarization-activated cyclic nucleotide-gated (HCN) channel by gaining access to a binding site within the open channel pore, and are removed from the blocking site by strong hyperpolarization with large inward I_f through the open channel. Cilobradine, compared to zatebradine blocks I_f more effectively and faster in both preparations. Consequently cilobradine strongly reduces the pacemaker diastolic depolarization rate and the cell's firing frequency.
© 2003 Elsevier B.V. All rights reserved.

Keywords: Cilobradine; Zatebradine; Pacemaker current (I_f); Use-dependence; HCN channel; (Electrophysiology)

1. Introduction

The molecular structure of the hyperpolarization-activated cyclic nucleotide-gated (HCN) channel, responsible for the cardiac pacemaker current (I_f), has been recently elucidated. The general structure of the HCN channel seems to be closely related to the structure of the different voltage-gated K^+ channels and the cyclic nucleotide-gated (CNG) channels. The α subunit of one monomer consists of six-transmembrane domains (S1 to S6), a pore loop between the S5 and S6 segments and a cyclic nucleotide-monophosphate (cNMP) binding domain in the C-terminal loop of the polypeptide (Kaupp and Seifert, 2001). Like the K^+ channels, the HCN channel presumably consists of a tetramere, constructed by the association of four α subunits plus various β subunits (Ulens and Tytgat, 2001; Yu et al., 2001). The exact composition of the wild HCN channel in both sino-atrial node and Purkinje cells is still not elucidated, because of the hetero-tetrameric structure of the α units and the presence of β subunits.

Bradycardiac agents are known to reduce the slope of the diastolic depolarization by blocking reversibly the I_f passing through the HCN channels (Kobinger, 1989; Kobinger and Lillie, 1984; Van Bogaert and Goethals, 1987). The drug, ZD7288, selectively blocks the cardiac I_f in isolated sino-atrial node cells (BoSmith et al., 1993) and Purkinje fibres (Berger et al., 1994, 1995). It has been shown in inside-out patches that ZD7288 blocks the mammalian HCN1 (mHCN1) channels by interacting with three amino acids located in the pore-lining S6 region after the open-channel configuration was induced by hyperpolarization (Ki Soon Shin et al., 2001). Although ZD7288 differs in some aspects regarding its mode of block of the HCN channels from what we know of zatebradine (UL-FS49) and cilobradine (DK-AH269) (see Section 4.1), this confirms our interpretation of the mechanism of I_f blockade by zatebradine in cardiac and neuronal HCN channels. The drug acts in the cationic form from the inside of the cell and can only gain access to the blocking binding site within the channel pore when the gate is open and the electrochemical gradient allows the entry of the positively charged drug into the channel. But at more negative voltages, with a large inward current crossing the open channel, the drug is swept from its binding site and relief from block is predominant (Goethals et al., 1993; Raes

* Corresponding author. Tel.: +32-3-218-0287; fax: +32-3-218-0326.
E-mail address: ppvbog@ruca.ua.ac.be (P.P. Van Bogaert).

0014-2999/$ - see front matter © 2003 Elsevier B.V. All rights reserved.
doi:10.1016/j.ejphar.2003.08.083

et al., 1998; Van Bogaert, 1989; Van Bogaert et al., 1990; Van Bogaert and Goethals, 1992). The same mechanism of interaction between the HCN channel of sino-atrial node cells and the bradycardiac agent, ivabradine (S16257), has been proposed recently (Bucchi et al., 2002). The relevance of I_f in the control of heart rate makes it an important pharmacological target. A reduced heart rate improves the myocardial energetic balance, because heart rate is tightly coupled with oxygen consumption (Braunwald, 1971). Furthermore, prolongation of the diastole duration, when the sinus rate is lowered, increases the coronary blood flow (Kedem et al., 1990). I_f is one of the many currents involved in cardiac and neural pacemaker mechanisms (DiFrancesco, 1993; Pape, 1996; Robinson and Siegelbaum, 2003). The bradycardiac agents, zatebradine and ivabradine (Bois et al., 1996; Thollon et al., 1994), induce a limited heart rate reduction (30% of the control) in a rate-dependent manner (Kobinger and Lillie, 1984). Zatebradine, cilobradine, DK-AH3 and ivabradine never cause sinus arrest and have limited or no negative inotropic side effects (Chen et al., 1992; Granetzy et al., 2000). Because of the presence of I_f in the retina (photoreceptors and ganglion cells) and in most neurons of both the central and peripheral nervous system (Biel et al., 2002; Moosmang et al., 2001; Santoro and Tibbs, 1999), it is important to characterise the potency and selectivity of bradycardiac agents. It is known that zatebradine blocks I_f both in photoreceptors and dorsal root ganglion neurons (Raes et al., 1998; Satoh and Yamada, 2002) at concentrations higher than those needed to block I_f in sino-atrial node cells. We now compare the I_f blockade by cilobradine, its stereoisomer, DK-AH268, and the racemic mixture, DK-AH3, with that by zatebradine, on both sheep Purkinje fibres and rabbit sino-atrial node cells. We conclude that cilobradine and its congeners are significantly more potent I_f blockers than zatebradine and all other bradycardiac agents. The mechanisms of this difference in potency are discussed.

2. Materials and methods

2.1. Description of the drugs tested

DK-AH269.Cl (cilobradine) is a white crystalline powder, soluble in water. The molecular weight is 519.1. The chemical name is: (*S*)-(+)-1,3,4,5-Tetrahydro-7,8-dimethoxy-3-((1-(2-(3,4-dimethoxyphenyl)-ethyl)-3-piperidinyl)-methyl)-2*H*-3-benzazepin-2-one-hydrochloride (pK_a = 8.60, log P = 1.17) (Fig. 1). The enantiomer of cilobradine is DK-AH268. The racemic mixture is DK-AH3.

UL-FS49.Cl (zatebradine) is a white crystalline powder, soluble in water. The molecular weight is 493.05. The chemical name is: 1,3,4,5-Tetrahydro-7,8-dimethoxy-3-(3-((2-(3,4-dimethoxyphenyl)-ethyl)-methylamino)propyl)-2*H*-3-benzazepin-2-one-hydrochloride (pK_a = 8.73, log P = 0.06) (Fig. 1).

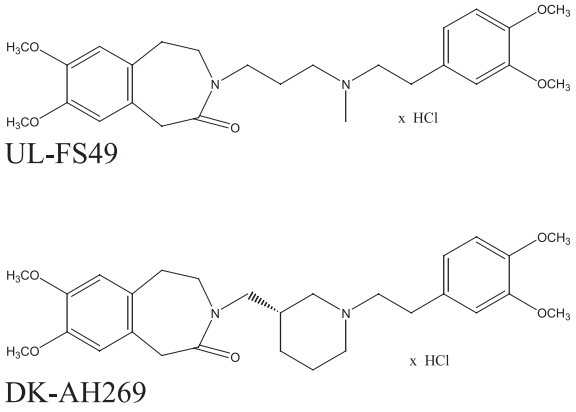

Fig. 1. Structural formula of zatebradine (UL-FS49) and cilobradine (DK-AH269).

A solution of these drugs has only a very small fraction of uncharged molecules (6% calculated value at pH 7.4 for cilobradine). The uncharged molecules are liposoluble and can diffuse through the plasma membrane.

With the intracellular pH in sheep Purkinje fibres at 7.2 (Ellis and Thomas, 1976; Roos and Boron, 1981) and the bath pH at 7.4, the intracellular concentration of the charged drug is substantially (50%) higher than the bath concentration ($[Drug^+]_i=([H^+]_i/(K_a+[H^+]_o))[Drug]_o$) with $[H^+]_i$ and $[H^+]_o$, respectively, the intra- and extracellular H^+ activity and K_a the acidity constant of the drug (Dr. Karl Thomae, Boehringer Ingelheim, Biberach, Deutschland kindly provided these drugs).

2.2. Experimental protocols

2.2.1. Experiments with Purkinje fibres

Experiments were carried out on short (1 mm) Purkinje strands from sheep heart with the two-microelectrode voltage-clamp technique as described earlier (Snyders and Van Bogaert, 1987; Van Bogaert et al., 1990). The fibres were cut and allowed to heal in high-K^+ (6 mM) Tyrode for 1 h. The temperature of the experimental chamber (volume 1.2 ml) was held at 39 ± 0.5 °C. The flow rate of the solution was 4 ml min^{-1}. A GeneClamp 500 (Axon Instruments) was used as voltage-clamp amplifier.

2.2.1.1. Experiments in normal Tyrode. Control action potentials were measured with the Purkinje fibres stimulated by a constant current pulse protocol (≈ 300 nA, 3 ms, 0.8 Hz) in normal Tyrode solution. The I_f properties were measured by application of rectangular voltage-clamp pulses of varying duration and varying amplitude in the pacemaker range (between −40 and −120 mV) starting from a holding potential (E_h) close to −80 mV at a pulse frequency of 0.04 Hz, allowing the tail current to recover completely. After the control run, the constant current pulse protocol was resumed in the presence of cilobradine until a stable reduction of the diastolic depolarization rate was observed (about 30 min to 1 h). A voltage-clamp run was made in the

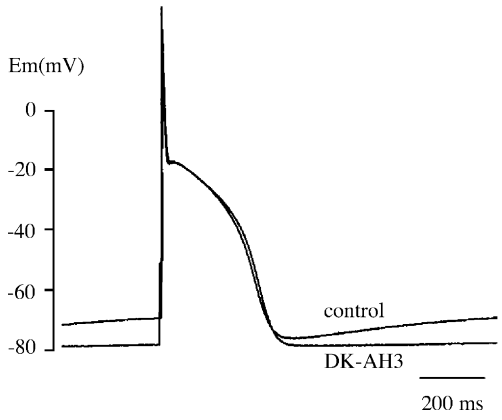

Fig. 2. Action potential during stimulation (constant current pulses: 300 nA, 3 ms, 0.8 Hz). Control action potential with a maximum diastolic depolarisation rate (DDR_{max}) of 20 mV s^{-1}. In the presence of DK-AH3 (0.3 μM), the resting membrane potential (E_r) remains constant at a more negative level due to the disappearance of the diastolic depolarisation.

presence of one and, if possible, a second concentration. Washout of the drug was not explored.

2.2.1.2. Experiments in modified Tyrode. The use-dependent blockade was induced by a pulse train (holding potential $E_h = -30$ mV, holding time 1.5 s; clamp potential $E_{cl} = -120$ mV, clamp time 1 s, N = number of pulses) after exposure to the drug for at least 30 min at E_h in modified Tyrode. The amplitude of I_f for each pulse was measured as the difference between the initial current after the capacitive transient, and the steady state current. The steady state fraction of blockade (b_{SS}) was defined as $b_{SS} = 1 - (i_{f_{ss}}/i_{f_0})$, $i_{f_{ss}}$ being the amplitude of I_f at steady state reduction and i_{f_0} the amplitude during pulse 1 (control). The rate constant λ_b of the exponential decline of I_f during one train was calculated for each pulse train. The results of different experiments (n) with the same drug concentration were averaged and S.E.M. was calculated. This procedure was used for a concentration range between 1 nM and 4 μM.

The recovery of the drug-induced blockade was measured by stopping the pulse protocol after steady state blockade had been reached and by clamping the membrane at different steady potentials ($E_{m,\ recovery}$) for a long time (Fig. 7A). The amplitude of I_f increased according to an exponential function with a rate constant $1/\tau_r$.

2.2.2. Experiments with cells isolated from rabbit sino-atrial node

The methods used to obtain and to voltage-clamp isolated rabbit sino-atrial node cells have been described previously (Goethals et al., 1993). A small (0.4 ml) Plexiglas chamber, with a heating plate in close contact with the bottom of the chamber (Van Ginneken and Giles, 1992), was used to record at 35 °C.

We used an Axoclamp-2A current- and voltage-clamp amplifier, Labmaster TL-1 DMA interface and pClamp6 software (Axon Instruments). Data were filtered with a Butterworth filter (Kemo, VBF 803). SigmaPlot5 (Jandel) was used for subsequent analysis. Membrane potentials and currents were recorded with the whole-cell variant of the patch-clamp technique (Hamill et al., 1981). Gigaohm seal formation (>10 GΩ) was monitored on a digital oscilloscope (Hewlett-Packard 54601 A). The membrane was ruptured by applying short suction. To reduce series-resistance problems, single-electrode voltage-clamp was performed in a discontinuous mode at a sampling rate of 5 kHz (30% duty cycle). The input of the sample-and-hold circuit was continuously monitored to ensure complete settling between current injection cycles. The liquid junction potential between the pipette solution and normal Tyrode solution was ±8 mV, for which the data were corrected.

2.3. Solutions

2.3.1. Experiments with Purkinje fibres

The composition of the normal Tyrode solution was as follows: NaCl 139 mM; KCl 4 mM; $CaCl_2$ 3.6 mM; $MgCl_2$

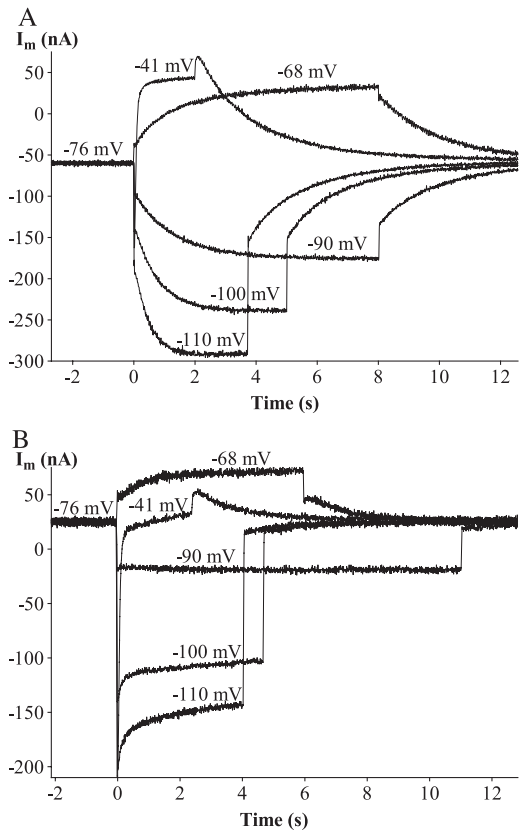

Fig. 3. Membrane currents at different voltage clamp potentials in normal Tyrode solution. (A) Control: the membrane current (I_m) at the holding potential ($E_h = -76$ mV) is inward. Two depolarizing steps (−68 and −41 mV) and three hyperpolarizing steps (−90, −100 and −110 mV) induced clear time-dependent currents followed by tail currents on return to the holding potential (same preparations as in Fig. 2). (B) With DK-AH3 (0.3 μM): I_m at E_h is outward; the time-dependent membrane currents at activation and deactivation were very small (note the larger I_m scale).

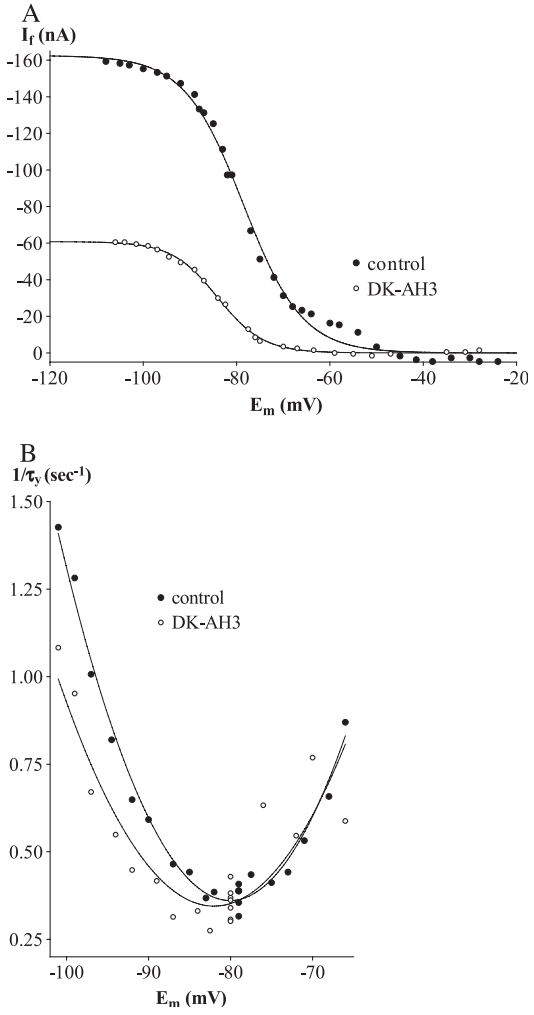

Fig. 4. (A) Steady state activation curve in normal Tyrode: control (filled symbols) and DK-AH3 (0.1 μM) (open symbols). $i_f = i_{f,\infty} - (i_{f,\infty}/(1 + e^{-(E_m - E_y/k)}))$. The drug reduced the amplitude of the steady state activation curve ($i_{f,\infty} = -162.5$ nA in control and -60.8 nA for DK-AH3) without a shift in half-maximal activation potential (E_y) or a difference in slope (k). (B) Inverse of time constants of activation ($1/\tau_y$) of I_f in normal Tyrode: control (filled symbols) and DK-AH3 (0.1 μM) (open symbols). There was no marked difference between control and drug.

1 mM; Glucose 5.5 mM. The solution was buffered with HEPES 10 mM and neutralised to pH 7.4 with NaOH.

The composition of modified Tyrode was the same but $BaCl_2$ 4 mM and $MnCl_2$ 2 mM were added. Mn^{2+} blocks $i_{Ca^{2+}}$, the slow inward Ca^{2+} current, Ba^{2+} eliminates i_{K_1}, the inward rectifying K^+ current, so that I_f becomes the most important fraction of the membrane current (i_m) at hyperpolarizing E_{cl} (DiFrancesco, 1981; DiFrancesco et al., 1984).

2.3.2. Experiments with cells isolated from rabbit sino-atrial node

The Tyrode solution was as follows: NaCl 140 mM; KCl 5.4 mM; $CaCl_2$ 1.8 mM; $MgCl_2$ 0.5 mM; glucose 10 mM. The solution was buffered with HEPES 5 mM and neutralized to pH 7.4 with NaOH. The internal pipette solution contained: KCl 20 mM; aspartic acid 110 mM; KOH 110 mM; $CaCl_2$ 0.5 mM; EGTA 3 mM; MgATP 5 mM; di-Tris phosphocreatine 2.5 mM; di-Na^+ phosphocreatine 2.5 mM, cAMP 0.05 mM; HEPES 5 mM; pH was adjusted to 7.2 with KOH.

The drugs were added to the Tyrode solution from a stock solution (1 μM in Tyrode). All solutions were pre-warmed to 35 °C and gassed with 100% O_2.

2.4. Statistical analysis

Data are shown as means ± S.E.M. for n experiments. To evaluate the statistical significance of differences of the means, we used Student's t-test for unpaired observations.

3. Results

3.1. Experiments with Purkinje fibres in normal Tyrode

3.1.1. Action potentials (Fig. 2)

Under control conditions, there was a clear diastolic depolarization (phase 4) with a maximum diastolic depolarization rate (DDR_{max}) of 20.3 mV s^{-1}. During continuous stimulation at 0.8 Hz in the presence of the drug, there was a progressive shift to a more negative maximal diastolic potential after the end of repolarization, with a gradual decrease of the maximal diastolic depolarization rate. As illustrated in Fig. 2, in the presence of 0.3 μM DK-AH3 the diastolic depolarisation was completely suppressed and the resting potential shifted to more negative voltages, without a significant change of the action potential shape or duration. The maximum diastolic depolariza-

Table 1
Effects of DK-AH3 (0.1 μM) in normal Tyrode solution

	DDR_{max}, mV s^{-1} (n)	E_r, mV (n)	R_{input}, kΩ (n)	E_y, mV (n)	$\bar{i}_f$, nA (n)	k, mV (n)	τ_y at E_h, s (n)	E_{thINa}, mV (n)	E_{thIto}, mV (n)
Control	20.3 ± 0.4 (8)	−71.1 ± 1.4 (11)	124 ± 15 (3)	−77.8 ± 3.6 (4)	−134 ± 26 (4)	8.1 ± 2.0 (4)	2.69 ± 0.11 (6)	−67 ± 2 (6)	−26 ± 1 (5)
[DK-AH3] 0.1 μM	3.2 ± 0.2 (8)*	−75.8 ± 0.8 (2)	171 ± 11 (3)*	−83.7 ± 2.5 (4)	−56 ± 11 (4)*	6.5 ± 0.4 (4)	2.85 ± 0.13 (7)	−69 ± 1 (3)	−27 ± 3 (2)

The maximal diastolic depolarization rate (DDR_{max}), the resting potential (E_r), the input resistance (R_{input}), the half-maximal activation potential (E_y), the amplitude ($\bar{i}_f$) and the slope factor (k) of the steady state activation curve, the time constant of the tail currents (τ_y), the threshold potential for the Na^+ current (E_{thINa}), the threshold potential for the transient outward K^+ current (E_{thIto}). The holding potential (E_h) was chosen close to the control resting potential (E_r). Results are expressed as mean values ± S.E.M. with the number of experiments (n).

* Significant difference between control and 0.1 μM DK-AH3 ($P < 0.05$, unpaired t-test, one-tailed).

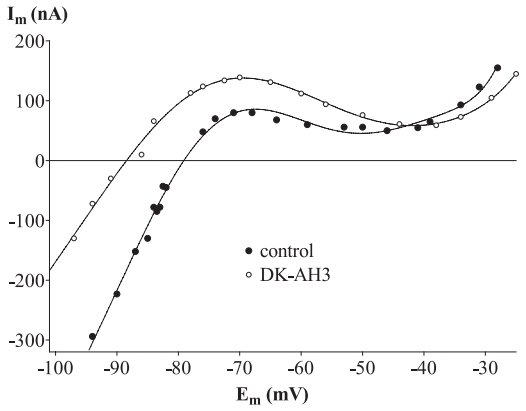

Fig. 5. Steady state current–voltage relation in normal Tyrode: control (filled symbols) and DK-AH3 (1 μM) (open symbols). The effect of DK-AH3 in the voltage range more negative to − 50 mV was an outward shift of I_m, a more negative resting potential ($E_{r,\ control} = -79.1$ mV, $E_{r,\ drug} = -88.5$ mV) and a decreased slope of the linear part of the curve, i.e. an increase in the membrane resistance ($R_{m,\ control} = 50.6$ kΩ, $R_{m,\ drug} = 73.0$ kΩ).

tion rate decreased gradually with increasing drug concentration and disappeared at 0.3 μM.

3.1.2. Membrane currents (Fig. 3)

The major current responsible for phase 4 of the action potential in Purkinje fibres is the time- and voltage-dependent I_f (DiFrancesco, 1994). Under control conditions (Fig. 3A), a hyperpolarizing step activated an increasing inward current with faster activation the more negative the clamp potential. Depolarizing steps elicited increasing outward currents. After termination of the voltage clamp pulse, tail currents on return to the holding potential saturated at the most de- and hyperpolarizing voltages. After the stabilisation of the effects of DK-AH3 (0.3 μM) on the action potential parameters, identical voltage-clamp pulses showed the following changes: the holding current shifted in the outward direction and the time- and voltage-dependent currents were strongly reduced in amplitude (Fig. 3B).

3.1.3. Gating properties of I_f (Fig. 4)

The steady state activation of I_f as a function of the membrane potential (E_m) can be fitted from the tail currents (i_f) as a Boltzmann curve $i_f = i_{f,\infty} - (i_{f,\infty}/(1 + e^{-(E_m - E_y/k)}))$ with $i_{f,\infty}$ the saturation value of the tail current, E_y the half-maximal activation potential and k the maximum slope at $E_m = E_y$. The effect of DK-AH3 (0.1 μM) was a reduction of the amplitude without a shift in the voltage dependence (E_y) or a difference in slope (k) (Fig. 4A and Table 1). The rate constant of activation ($1/\tau_y$) plotted at different membrane potentials shows no difference between control and drug (Fig. 4B). The lowest rate constant was measured at the half-maximal activation potential (E_y). These observations indicate that there were no significant modifications in the voltage-dependence or in the kinetics of the gating mechanism of the I_f (Table 1).

3.1.4. Steady state current–voltage relation (Fig. 5)

The steady state current–voltage relation under control conditions is the typical N-shaped curve with a resting

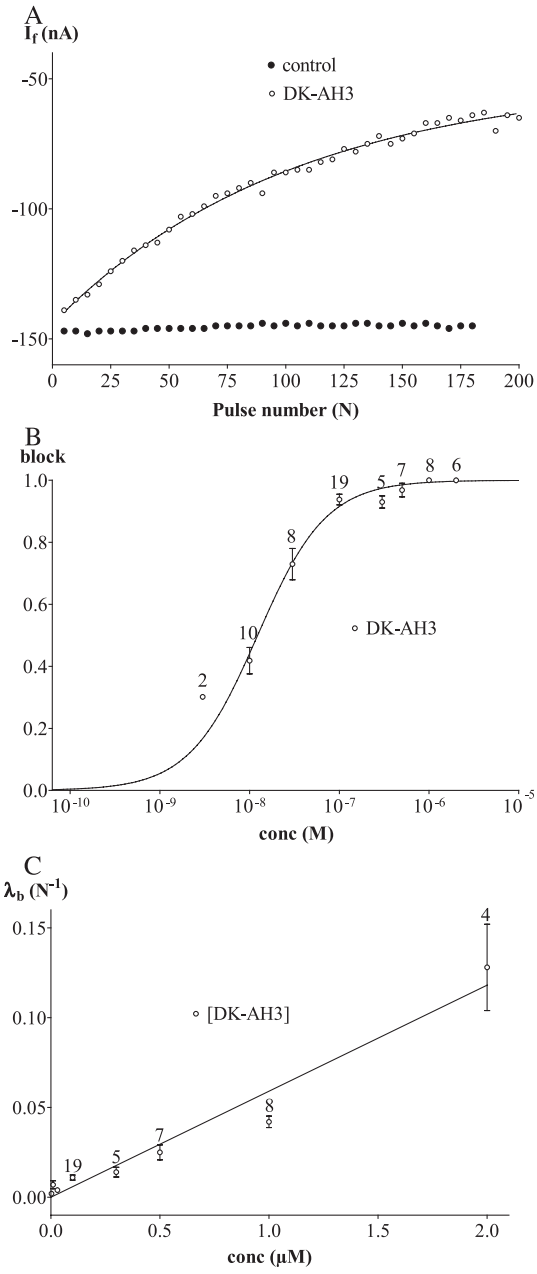

Fig. 6. (A) Induction of use-dependent blockade. I_f as a function of the number of pulses (N) of a blocking train: control (filled symbols) and DK-AH3 (30 nM) (open symbols). The blockade appeared as an exponential function of N: $i_f = i_{f_{SS}} + (i_{f_0} - i_{f_{SS}})e^{-(N/\tau)}$. ($i_{f_{SS}}$ is the steady state I_f, i_{f_0} is the control I_f). Under control conditions, no block appeared ($I_f = -146 \pm 2$ nA; 180 pulses); in the presence of the drug a steady state blockade ($b_{SS} = 1 - (i_{f_{SS}}/i_{f_0})$) of 0.73 was induced with a pulse constant $\tau_b = 104$ pulses (rate constant $\lambda_b = 0.010\ N^{-1}$). (B) Dose–response curve: steady state block (b_{SS}) of I_f in function of [DK-AH3] after blocking train at 0.04 Hz. The curve fits the function $b_{SS} = (1/(1 + (K_d/[D])^{n_H}))$ with $K_d = 12.3$ nM and $n_H = 1.14$ ($r^2 = 0.996$). (C) The rate constant of blockade (λ_b) as a function of [DK-AH3]. The curve fits a straight line with intercept = 0.002 N^{-1} and slope = 0.0542 N^{-1} μM^{-1} ($r^2 = 0.936$).

potential (E_r) at −79.1 mV. In the presence of 1 μM DK-AH3, the E_r shifted to more negative voltages (−88.5 mV) as the result of an outward shift of the membrane currents negative to −50 mV (Fig. 5). In the range of inward currents, the slope of the linear part is less steep in the presence of the drug, indicating an increase in membrane input resistance (R_m): $R_{m,\ control} = 50.6$ kΩ, $R_{m,\ drug} = 73.0$ kΩ. The threshold potentials (E_{th}) for I_{Na} and I_{to} (transient outward K^+ current) were not changed (Table 1).

3.2. Experiments with Purkinje fibres in modified Tyrode

3.2.1. Induction of use-dependent blockade (Fig. 6)

In previous experiments, we have demonstrated that both zatebradine and cilobradine cause a use-dependent block of I_f in cardiac Purkinje fibres, isolated rabbit sino-atrial node cells and the I_h current in nerve cells (Goethals et al., 1993; Raes et al., 1998; Van Bogaert and Raes, 1991; Van Bogaert et al., 1990). A voltage pulse to −120 mV fully activates I_f with a time constant (τ_y) of 258 ± 14 ms ($n = 8$). On return to the E_h at −30 mV, the I_f deactivates with a time constant (τ_y) of 74 ± 13 ms ($n = 8$). Based on the experiments under control conditions, only those with a control I_f (i_{f_0}) between 50 and 250 nA and greater than the leak current were used. The steady state I_f, measured after a 1-s pulse from −30 to −120 mV at a rate of 0.4 Hz, is plotted as a function of the pulse number in the train (Fig. 6A). In the absence of the drug, there was no decline in the amplitude of I_f during the train ($I_f = -146 \pm 2$ nA; $N = 180$ pulses). After 30 min in the presence of the drug (DK-AH3, 30 nM) at −30 mV, the pulse train was resumed and there was an exponential decline in the amplitude of I_f to a steady state value ($i_{f_{SS}}$). The amplitude of I_f at the first pulse (i_{f_0}) may be considered as control pulse because no marked blocking effect appeared during the diffusion period at −30 mV of sub-micromolar concentrations of the drug as described for zatebradine (Van Bogaert et al., 1990). At this concentration, the steady state fraction of blockade (b_{SS}) was

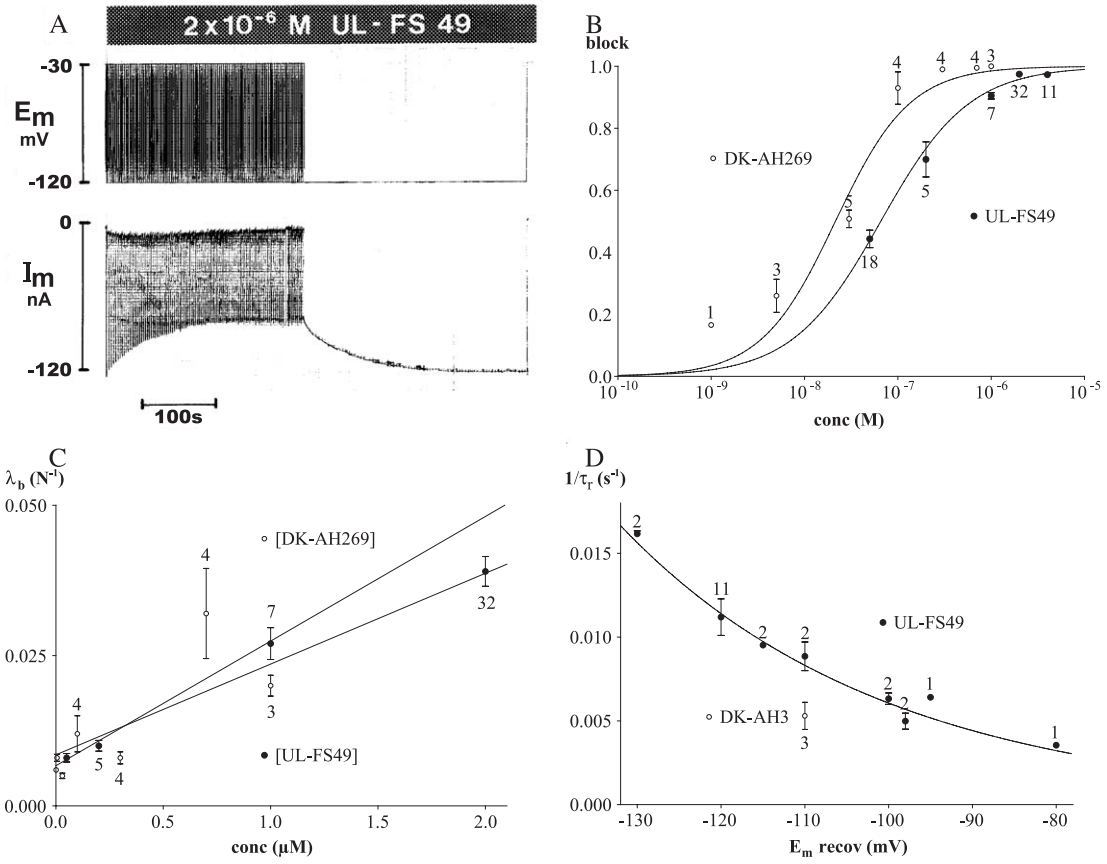

Fig. 7. (A) Decrease of I_f in the presence of 2 μM zatebradine (UL-FS49) during the pulse train at 0.4 Hz (holding potential $E_h = -30$ mV, 1.5 s; clamp potential $E_{cl} = -120$ mV, 1 s; $N = 110$ pulses) followed by a slow exponential recovery of the inward current during a prolonged hyperpolarizing pulse ($E_{cl} = -120$ mV, 320 s). I_m is the total membrane current. (B) Dose–response curve (Hill plot) of cilobradine (DK-AH269) and zatebradine (UL-FS49) after blocking train at 0.4 Hz. The $K_d = 21.4$ nM and the slope = 1.09 for cilobradine (open symbols), the $K_d = 65.6$ nM and the slope = 0.92 for zatebradine (filled symbols). (C) Rate constant of blockade (λ_b) as a function of drug concentration. The results fit a straight line with intercept = 0.007 N^{-1} and slope = 0.0207 N^{-1} μM^{-1} for cilobradine (DK-AH269) and intercept = 0.009 N^{-1} and slope = 0.0150 N^{-1} μM^{-1} for zatebradine (UL-FS49). (D) Rate constant of unblock ($1/\tau_r$) as function of recovery membrane potential ($E_{m,\ recovery}$). The results for zatebradine (UL-FS49) fit an exponential curve $\left(y = ae^{\left(-\frac{x}{b}\right)}\right)$ with $a = 0.00026$ s^{-1}, $b = 32$ mV. At −110 mV, the rate constant of unblock ($1/\tau_r$) in the presence of DK-AH3 was lower.

Table 2
Fraction and rate constant of blockade

Drug	Experiments	b_{SS}		λ_b	
	n	K_d (nM)	n_H	Slope (N^{-1} μM^{-1})	Intercept (N^{-1})
DK-AH268	109	21.3 ± 2.4	0.62 ± 0.04	0.0154 ± 0.0010	0.011 ± 0.002
DK-AH269	24	21.4 ± 2.9	1.09 ± 0.15	0.0207 ± 0.0049	0.007 ± 0.002
DK-AH3	65	12.3 ± 1.0	1.14 ± 0.10	0.0542 ± 0.0034	0.002 ± 0.002
UL-FS49	73	65.6 ± 0.4	0.92 ± 0.06	0.0150 ± 0.0094	0.009 ± 0.002

Hill plot $b_{SS} = (1/(1 + (K_d/[D])^{n_H}))$ of steady state fraction of blockade (b_{SS}) and linear plot of rate constant of blockade (λ_b) as a function of the concentration. K_d is the concentration of drug for 50% b_{SS} and n_H is the slope factor for $[D] = K_d$. DK-AH269 is cilobradine and UL-FS49 is zatebradine. Significant difference between all K_d's ($P < 0.0001$) except between DK-AH268 and DK-AH269 ($P = 0.98$) (unpaired t-test, two-tailed).

0.73 ± 0.05 ($n = 8$) and the rate constant of blockade λ_b was 0.004 ± 0.001 N^{-1} ($n = 8$).

As described previously for zatebradine, the steady state fraction of blockade increased sigmoidally as a function of the logarithm of the drug concentration [D]: $b_{SS} = (1/(1 + (K_d/[D])^{n_H}))$ with K_d the concentration of drug for 50% b_{SS} and n_H the slope factor for $[D] = K_d$ (Figs. 6B and 7B). The results of this Hill plot are shown in Table 2. There is no significant difference between cilobradine and DK-AH268, but there is a significant difference in K_d between all the other drugs ($P <$ 0.0001). The rate constant for blockade increased linearly with the drug concentration: $\lambda_b = a + b[D]$ (Fig. 6C and Table 2). The results are given in Table 2.

3.2.2. Removal of blockade and comparison between zatebradine and DK-AH3

After induction of use-dependent block by the bradycardiac agent, zatebradine, or DK-AH3, the amplitude of I_f decreased to a fraction of the control value at the beginning of the pulse train. When the membrane potential was held at − 120 mV after the last pulse of the train, a slow exponentially increasing inward current was measured (Fig. 7A). The unblocking process, measured under the same experimental conditions for zatebradine and DK-AH3, shows that the rate of unblock ($1/\tau$) was significantly slower ($P < 0.05$) when DK-AH3 was present: $1/\tau$ at − 110 mV is 0.0053 ± 0.0014 s^{-1} ($n = 3$) for DK-AH3 and 0.0089 ± 0.0012 s^{-1} ($n = 3$) in the case of zatebradine (Fig. 7D). Application of a test pulse

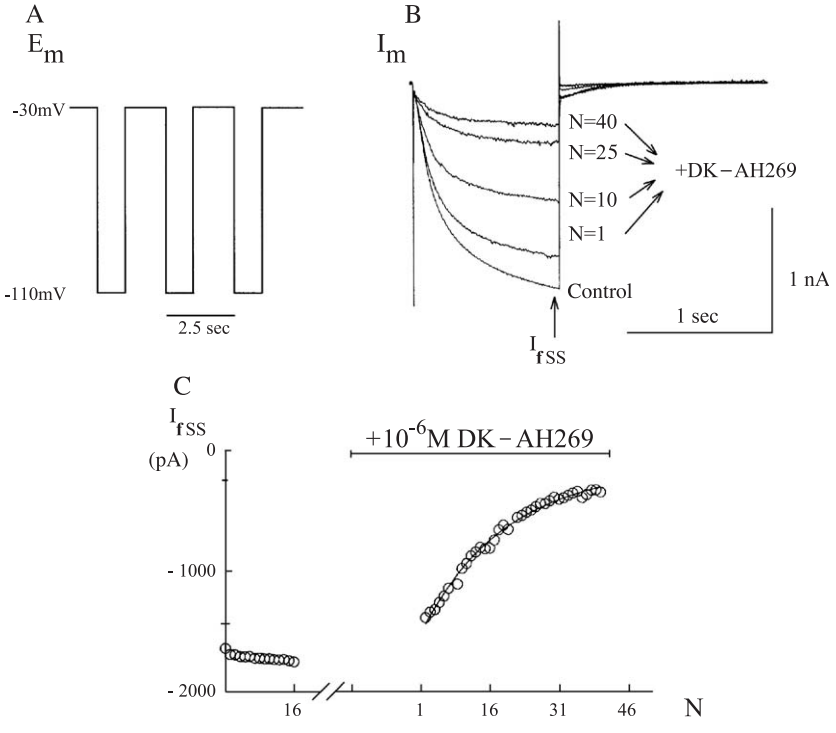

Fig. 8. Block by cilobradine (DK-AH269) (1 μM) in cells isolated from the rabbit sino-atrial node. (A) The use-dependent blockade was induced by a pulse train (holding potential $E_h = -30$ mV, 1.5 s; clamp potential $E_{cl} = -110$ mV, 1 s, N = pulse number) after exposure to the drug for at least 30 min at E_h in normal Tyrode. (B) I_f samples during blocking train (I_{fSS} is the steady state amplitude of I_f after activation. (C) Exponential decrease of I_{fSS} during pulse train. Steady state block (b_{SS}) = 91.4% and rate constant of block (λ_b) = 0.060 N^{-1}. The difference in amplitude of the I_f between the last control pulse and the first test pulse of the train ($N = 1$) is due to run-off of the current.

from −30 to −120 mV, applied after completion of recovery, activated a clear time-dependent I_f, indicating that the increase in current was the result of the unblocking process, and not simply an increase in leak current. Reapplication of a pulse train resulted in the reappearance of the use-dependent blockade (not shown).

3.3. Experiments on isolated rabbit sino-atrial cells

On hyperpolarization of the cell membrane from −30 to −110 mV, a large, slowly increasing, inward pacemaker current was measured. At repolarization to −30 mV, a decreasing inward tail current followed the deactivation of the I_f conductance at a potential below its reversal potential (Fig. 8A and B). Under control conditions, the peak amplitude of the I_f was −1750 pA in this cell and stayed constant during a voltage-clamp pulse train at 0.4 Hz (16 pulses). After 30 min at −30 mV in the presence of 1 μM cilobradine, we reapplied the pulse train and the peak I_f declined exponentially with a rate constant of $\lambda_b = 0.060$ N^{-1} to 8.6% of the control value (Fig. 8C). Cilobradine (1 μM) induced 82 ± 3% ($n = 5$) use-dependent blockade of the I_f with a pulse rate constant $\lambda = 0.069 \pm 0.004$ N^{-1} ($n = 5$). The use-dependent blockade induced by cilobradine was nearly completely reversed without washout of the drug by a long hyperpolarization at −100 mV with a rate constant $1/\tau_r = 0.027$ s^{-1}. After the recovery from block, a second pulse train reinduced use-dependent block. The speed and extent of unblock was greater the more negative was the recovery holding potential (not shown).

4. Discussion

4.1. I_f affecting drugs

I_f in cardiac tissues (I_h in nerve cells) is affected by a number of drugs. Some, like alinidine (Snyders and Van Bogaert, 1987) and ZD7288 (BoSmith et al., 1993), block the current without any use and frequency dependence (class 1). These drugs not only can presumably block the HCN channels in the closed state, at a holding potential of −30 mV, but are also active in cationic form from the inside on an open channel at mild hyperpolarization (Harris and Constanti, 1995; Shin et al., 2001). Strong hyperpolarization to negative potentials rapidly removes the block caused by ZD7288 with a time constant of 2.1 s in sheep cardiac Purkinje fibres (Berger et al., 1995). Direct application of ZD7288 to an inside-out patch, expressing mHCN1 channels, demonstrates a steep voltage dependence of the block, roughly corresponding to the mirror image of the voltage dependence of the I_f gating mechanism (Shin et al., 2001). These observations indicate that the cationic drug can access the channel both in the open and closed states but that access is hindered by the electric field, favouring unblock at strong hyperpolarization.

Ivabradine and zatebradine form another class of drugs, chemically related to the Ca^{2+}-channel blocking drugs, verapamil and falipamil (class 2). These drugs are characterised by a use- and voltage-dependent blocking process (Bois et al., 1996; Bucchi et al., 2002; Goethals et al., 1993; Pape, 1994; Raes et al., 1998; Van Bogaert et al., 1990). The crucial difference in the mode of action is that these drugs can only gain access to the blocking site within the channel when the activation gate is in the open configuration while the other drugs (class 1) presumably also block the channel in closed configuration.

We have accumulated data indicating that cilobradine has use-dependent blocking properties comparable to those of zatebradine but with some clear differences, especially as the potency of the drug is concerned, both in Purkinje fibres and in sino-atrial node cells.

4.2. Experiments on sheep Purkinje fibres in normal Tyrode

Reduction of I_f is the main effect of the racemic mixture, DK-AH3, as well as of the two stereoisomers, DK-AH268 and DK-AH269 (cilobradine). Selective suppression of the inward I_f abolishes the diastolic depolarization and shifts the resting potential to a voltage close to the maximal diastolic potential, without modification of the other phases of the action potential (Noble, 1984). This was shown clearly in our experiment with 0.3 μM DK-AH3 (Fig. 2). In normal Tyrode, the action of both DK-AH3 and cilobradine can be explained mostly by a potent blockade of I_f. This is evident from the voltage-clamp measurements in the pacemaker voltage range: the slowly activating and deactivating current was almost completely abolished with 0.3 μM DK-AH3 (Fig. 3). The outward shift of the membrane current in the steady state current–voltage relation at voltages negative to −50 mV in the presence of 1 μM DK-AH3, resulting in a more negative resting potential, can either be caused by an increase in outward current or a decrease in inward current. In view of our results, it appears that this shift is caused by the reduction of the steady state inward I_f in the pacemaker range (Fig. 5). This also explains the higher membrane resistance at potentials negative to the resting potential (Table 1). In the submicromolar concentration range used in our experiments, no other currents are affected: the threshold voltages of both I_{Na}, the fast inward Na^+-current responsible for the fast upstroke of the action potential, and I_{to}, the transient outward K^+-current responsible for the fast (phase 1) repolarization after the spike were not significantly changed, nor was there any influence of either compound on phase 0 or 1 of the action potential (Table 1 and Fig. 2).

4.3. Use-dependent blockade of I_f in Purkinje fibres

Use-dependent blockade was investigated in a Tyrode solution containing $BaCl_2$ and $MnCl_2$ to completely block I_{Ca} and I_{K1}. This solution closely resembles the normal Tyrode solution. Because the Na^+ and K^+ content of the

extracellular solution greatly affects I_f conductance (DiFrancesco, 1981) and because the kinetics of unblock by zatebradine are very sensitive to the amount of current flowing at −120 mV (Van Bogaert, 1989, 1994, 1999; Van Bogaert et al., 1990), it is important to compare these drug effects, not only using the same voltage protocols, but also under similar ionic conditions. This is illustrated by the shift to lower values of the unblocking rate constants at −120 mV in the presence of zatebradine in Tris-substituted low-Na^+ (35 mM) solution ($1/\tau_r = 0.0055\ s^{-1}$) compared with the unblocking rate constants in normal Na^+ (144 mM) solution ($1/\tau_r = 0.0112\ s^{-1}$) (Fig. 9B in Van Bogaert et al., 1990 and Fig. 7D in the present paper). To bind with the receptor, the channel gate must be in the open position because, no matter how long the preparations are exposed to the drug at a resting potential of −30 mV in modified Tyrode, we always measured a distinctly large inward time-dependent I_f on application of the first pulse of the train. Thus, there was no apparent tonic block by cilobradine or DK-AH3 in the concentration ranges (1 nM–1 μM for cilobradine and 3 nM–2 μM for DK-AH3) we used in the experiments.

A necessary, but not solely sufficient, condition for drug action is that the I_f channel be switched in the open state by shifting the voltage in the range of activation of I_f. Although at −120 mV, the HCN channel activation gate is open, the electrochemical gradient is not favourable for a positively charged drug to move from the cytoplasm into the channel pore. We therefore speculate that drug access to the binding site mostly takes place when the voltage is stepped back to −30 mV and the channel takes some time to close at a voltage more favourable for the drug to gain access to the binding site (Bucchi et al., 2002; Goethals et al., 1993; Van Bogaert et al., 1990). On the other hand, unblock occurs mainly at very negative membrane potentials when the channels are in open conformation, with large inward I_f and a strong transmembrane electrical field, favouring the exit of cationic molecules out of the open channel into the cytosol.

DK-AH3 induces a use-dependent blockade of I_f that is both stronger and faster compared to that with zatebradine. The unblocking process, measured under the same experimental conditions (−110 mV), was significantly slower with DK-AH3 than with zatebradine (Fig. 7D). Also, partial results obtained at other membrane potentials confirm that the rate constants of unblock are clearly smaller in the presence of cilobradine or DK-AH3 than with zatebradine. In a number of experiments, a test pulse to −120 mV was applied after completion of recovery. This pulse evoked the reappearance of a clear time-dependent inward current. This confirms the reality of recovery from block and disproves an increase in leak current during the prolonged hyperpolarization. Unfortunately, this protocol could not be applied systematically to confirm unambiguously the unblocking process because many preparations deteriorated during the very long hyperpolarization (several minutes) needed to unblock the channels in the presence of cilobradine. A significantly slower dissociation rate constant for DK-AH3 can partly explain the stronger blocking effect of DK-AH3 and cilobradine on I_f compared to the blocking effect of zatebradine.

In the framework of the guarded receptor theory (Starmer and Grant, 1985), the rate of current decline during a pulse train (λ_b) is linearly related to the drug concentration, with the slope proportional to the association rate constant of the drug for the receptor (see discussion in Van Bogaert et al., 1990). The slope of the relation is higher with DK-AH3 and cilobradine, which can be interpreted as the consequence of a higher association rate for the binding site in the HCN channel of these drugs compared to that for zatebradine.

4.4. Experiments with isolated rabbit sino-atrial node cells

A limited number of experiments on the action of cilobradine on isolated rabbit sino-atrial node cells were performed under conditions practically identical to those described for zatebradine (Goethals et al., 1993). Cilobradine (1 μM) induced a greater [82 ± 3% ($n = 5$)] and faster [$\lambda = 0.069 \pm 0.004\ N^{-1}$ ($n = 5$)] use-dependent blockade of the I_f than seen with a steady state block of 36 ± 5% ($n = 11$) and $\lambda = 0.013 \pm 0.003\ N^{-1}$ ($n = 11$) in the presence of the same amount of zatebradine (Goethals et al., 1993). With the same concentration of ivabradine (1 μM), the I_f block was both smaller [32 ± 6% ($n = 3$)] and slower (calculated pulse rate constant of $0.044\ N^{-1}$) (Bois et al., 1996; Bucchi et al., 2002). From these data, we can conclude that cilobradine blocks the I_f in sino-atrial node cells more effectively than all bradycardiac agents described so far. One of the factors explaining this difference in I_f blocking potency is presumably the fact that the recovery from use-dependent block has a time constant of 7.0 ± 0.5 s ($n = 6$) at −100 mV for ivabradine and 37 ± 10 s ($n = 3$) at −110 mV in the case of cilobradine.

4.5. Conclusion

Cilobradine and DK-AH3 are drugs that bind on a receptor in the I_f channels in cardiac pacemaker tissue and block these channels, decreasing the diastolic depolarization rate. These drugs presumably act on the I_f channel in the same way as does zatebradine. One intracellular cilobradine cationic molecule blocks one I_f channel in an all-or-none manner. The binding site is located within the I_f channel pore and can be reached by a hydrophilic pathway from the inside of the cell, provided the channel is in the open configuration and a favourable electrical field is present.

Unblock of the channel occurs preferentially in the open I_f channel configuration and is enhanced by very negative E_m and by inward currents crossing the open channel. There is no significant difference in action between the two stereoisomers, cilobradine (DK-AH269) and DK-AH268.

The same was observed for the stereoisomers of ivabradine ((+)-S16257) and (−)-S16260 (Thollon et al., 1997).

The stronger blocking potency and the faster rate of blocking of DK-AH3 and cilobradine compared to those of zatebradine in both Purkinje fibres and isolated rabbit sino-atrial cells is presumably the consequence of a slower dissociation rate, as measured directly under similar conditions, and also probably of a higher association rate, but this could not be measured in a direct way. The dissociation rate constant of ivabradine is more than six-fold less than of cilobradine at a holding potential of −100 mV (Bucchi et al., 2002). This can explain the stronger I_f blockade by cilobradine.

I_f in sheep cardiac Purkinje fibres is more sensitive to blockade by DK-AH3, cilobradine and zatebradine than I_f in sino-atrial node cells. The use-dependent blockade by zatebradine of I_f from rabbit sino-atrial node cells under comparable experimental conditions has an apparent K_d of 480 nM (Goethals et al., 1993), seven times greater than in Purkinje fibres (K_d of 66 nM). Part of the difference is presumably related to the rate of recovery from block, which is one order of magnitude faster in sino-atrial node cells (DiFrancesco, 1994; Goethals et al., 1993). Another factor could be that the HCN in sino-atrial node cells and Purkinje fibres are constituted by different heteromers (Yu et al., 2001). The HCN4 isoform, which is present in Purkinje fibres, has much slower kinetics of I_f deactivation. This could result in longer open times at −30 mV for the block by zatebradine and cilobradine to take place.

Acknowledgements

This work was supported by the Born-Bunge Foundation (Cardiovascular section) and by Boehringer Ingelheim Pharma (Germany).

References

Berger, F., Borchard, U., Gelhaar, R., Hafner, D., Weis, T., 1994. Effects of the bradycardic agent ZD 7288 on membrane voltage and pacemaker current in sheep cardiac Purkinje fibres. Naunyn-Schmiedeberg's Arch. Pharmacol. 350, 677–684.

Berger, F., Borchard, U., Gelhaar, R., Hafner, D., Weis, T.M., 1995. Inhibition of pacemaker current by bradycardic agent ZD 7288 is lost use-dependently in sheep cardiac Purkinje fibres. Naunyn-Schmiedeberg's Arch. Pharmacol. 353, 64–72.

Biel, M., Scheider, A., Wahl, C., 2002. Cardiac HCN channels: structure, function, and modulation. Trends Cardiovasc. Med. 12, 206–213.

Bois, P., Bescond, J., Renaudon, B., Lenfant, J., 1996. Mode of action of bradycardic agent, S16257, on ionic currents of rabbit sino-atrial node cells. Br. J. Pharmacol. 118, 1051–1057.

BoSmith, R.E., Briggs, I., Sturgess, N.C., 1993. Inhibitory actions of ZENECA ZD7288 on whole-cell hyperpolarization activated inward current (I_f) in guinea pig dissociated sino-atrial node cells. Br. J. Pharmacol. 110, 343–349.

Braunwald, E., 1971. Control of myocardial oxygen consumption. Am. J. Cardiol. 27, 416–432.

Bucchi, A., Baruscotti, M., diFrancesco, D., 2002. Current-dependent block of rabbit sino-atrial node I_f channels by ivabradine. J. Gen. Physiol. 120, 1–13.

Chen, J.S., Wang, W., Cornish, K.G., Zucker, I.H., 1992. Baro- and ventricular reflexes in conscious dogs subjected to chronic tachycardia. Am. J. Physiol., Heart Circ. Physiol. 263, 1084–1089.

DiFrancesco, D., 1981. A study of the ionic nature of the pacemaker current in calf Purkinje fibres. J. Physiol. 314, 377–393.

DiFrancesco, D., 1993. Pacemaker mechanisms in cardiac tissue. Annu. Rev. Physiol. 55, 455–472.

DiFrancesco, D., 1994. Some properties of the UL-FS49 block of the hyperpolarization-activated (I_f) current in sino-atrial myocytes. Pflugers Arch. 427, 64–70.

DiFrancesco, D., Ferroni, A., Visentin, S., 1984. Barium-induced blockade of the inward rectifier in calf Purkinje fibres. Pflugers Arch. 402, 446–453.

Ellis, D., Thomas, R.C., 1976. Microelectrode measurement of the intracellular pH of mammalian heart cells. Nature 262, 224–225.

Goethals, M., Raes, A., Van Bogaert, P.P., 1993. Use-dependent block of the pacemaker current I_f in rabbit sino-atrial node cells by zatebradine (UL-FS 49). Circulation 88, 2389–2401.

Granetzy, A., Schwanke, U., Gams, E., Schipke, J.D., 2000. Effects of a bradycardic agent (DK-AH269) on haemodynamics and oxygen consumption of isolated blood-perfused rabbit hearts. J. Clin. Basic Cardiol. 3, 191–196.

Hamill, O.P., Marty, A., Neher, E., Sakmann, B., Sigworth, F.J., 1981. Improved patch clamp techniques for high-resolution current recordings from cells and cell-free membrane patches. Pflugers Arch. 391, 85–100.

Harris, N.C., Constanti, A., 1995. Mechanisms of block by ZD7288 of the hyperpolarization-activated inward rectifying current in guinea pig substantia nigra neurons in vitro. J. Neurophysiol. 74, 2366–2378.

Kaupp, B., Seifert, R., 2001. Molecular diversity of pacemaker ion channels. Annu. Rev. Physiol. 63, 235–257.

Kedem, J., Acad, B.A., Weiss, H.R., 1990. Pacing during reperfusion elevates regional myocardial oxygen consumption. Am. J. Physiol., Heart Circ. Physiol. 259, 872–878.

Kobinger, W., 1989. Specific bradycardic agents. In: Vaughan Williams, E.M., Campbell, T.J. (Eds.), Handb. Exp. Pharmacol., vol. 89. Springer Verlag, Berlin Heidelberg.

Kobinger, W., Lillie, C., 1984. Cardiovascular characterization of UL-FS 49, 1,3,4,5-tetrahydro-7,8-dimethoxy-3-[3-[[2-(3,4-dimethoxyphenyl) ethyl]methylimino]propyl]-24-3-benzazepin-2-on hydrochloride, a new 'specific bradycardic agent'. Eur. J. Pharmacol. 104, 9.

Moosmang, S., Stieber, J., Zong, X., Biel, M., Hofmann, F., Ludwig, A., 2001. Cellular expression and functional characterization of four hyperpolarization-activated pacemaker channels in cardiac and neuronal tissues. Eur. J. Biochem. 268, 1646–1652.

Noble, D., 1984. The surprising heart: a review of recent progress in cardiac electrophysiology. J. Physiol. 353, 1–50.

Pape, H.C., 1994. Specific bradycardic agents block the hyperpolarization-activated cation current in central neurons. Neuroscience 59, 363–373.

Pape, H.C., 1996. Queer current and pacemaker: the hyperpolarization-activated cation current in neurons. Annu. Rev. Physiol. 58, 299–327.

Raes, A., Van de Vijver, G., Goethals, M., Van Bogaert, P.P., 1998. Use-dependent block of I_h in mouse dorsal root ganglion neurons by sinus node inhibitors. Br. J. Pharmacol. 125, 741–750.

Robinson, R., Siegelbaum, S., 2003. Hyperpolarization-activated cation currents: from molecules to physiological function. Annu. Rev. Physiol. 65, 453–480.

Roos, A., Boron, F., 1981. Intracellular pH. Physiol. Rev. 61, 2.

Santoro, B., Tibbs, G., 1999. The HCN gene family: molecular basis of the hyperpolarization-activated pacemaker channels. Ann. N.Y. Acad. Sci. 868, 741–764.

Satoh, T.O., Yamada, M., 2002. Multiple inhibitory effects of zatebradine

(UL-FS49) on the electrophysiological properties of retinal rod photoreceptors. Eur. J. Physiol. 443, 532–540.

Shin, H., Rothberg, B.S., Yellen, G., 2001. Blocker state dependence and trapping in hyperpolarization-activated cation channels: evidence for an intracellular activation gate. J. Gen. Physiol. 117, 91–102.

Snyders, D.J., Van Bogaert, P.P., 1987. Alinidine modifies the pacemaker current in sheep Purkinje fibres. Pflugers Arch. 410, 83–91.

Starmer, C.F., Grant, A.O., 1985. A. Phasic ion channel blockade. A kinetic model and parameter estimation procedure. Mol. Pharmacol. 28, 348–356.

Thollon, C., Cambarrat, C., Vian, J., Prost, J.F., Peglio, J.L., Vilaine, J.P., 1994. Electrophysiological effects of S16257, a novel sino-atrial modulator on rabbit and guinea-pig cardiac preparations. Br. J. Pharmacol. 112, 37–42.

Thollon, C., Bidouard, J.P., Cambarrat, C., Lesage, L., Reure, H., Delescluse, I., Vian, J., Peglion, J.L., Vilaine, J.P., 1997. Stereospecific in vitro and in vivo effects of the new sinus node inhibitor (+)-S16527. Eur. J. Pharmacol. 339, 43–51.

Ulens, C., Tytgat, J., 2001. Functional heteromerization of HCN1 and HCN2 pacemaker channels. J. Biol. Chem. 276, 6069–6072.

Van Bogaert, P.P., 1989. Extracellular caesium accelerates the onset of use-dependent I_f pacemaker current blockade. Biophys. J. 55, 291a.

Van Bogaert, P.P., 1994. Recovery from block by zatebradine of the I_f current in isolated sheep cardiac Purkinje fibres. J. Physiol. 479 (124 pp.).

Van Bogaert, P.P., 1999. I_f current blockade by UL-FS49 is relieved by a current dependent process in sheep cardiac Purkinje fibers. Pflugers Arch. 437, R6.

Van Bogaert, P.P., Goethals, M., 1987. Pharmacological influence of specific bradycardic agents on the pacemaker current of sheep cardiac Purkinje fibres. A comparison between three different molecules. Eur. Heart J. 8, L35–L42.

Van Bogaert, P.P., Goethals, M., 1992. Blockade of the pacemaker current by intracellular application of UL-FS49 and UL-AH99 in sheep cardiac Purkinje fibers. Eur. J. Pharmacol. 229, 55–62.

Van Bogaert, P.P., Raes, A., 1991. Use-dependent blockade of the I_f current by DK-AH3 in sheep Purkinje fibres: kinetic characteristics. Arch. Int. Pharmacodyn. 310, 191.

Van Bogaert, P.P., Goethals, M., Simoens, C., 1990. Use- and frequency-dependent blockade by UL-FS49 of the I_f pacemaker current in sheep cardiac Purkinje fibres. Eur. J. Pharmacol. 187, 241–256.

Van Ginneken, A.C.G., Giles, W., 1992. Voltage-clamp measurements of the hyperpolarization-activated inward current I_f in single cells from rabbit sino-atrial node. J. Physiol. 434, 57–83.

Yu, H., Wu, I., Potapova, I., Wymore, R.T., Holmes, B., Zuckerman, J., Pan, Z., Wang, H., Shi, W., Robinson, R.B., El-Maghrabi, M.R., Benjamin, W., Dixon, J., McKinnon, D., Cohen, I.S., Wymore, R., 2001. MinK-related peptide 1. A β subunit for the HCN ion channel subunit family enhances expression and speeds activation. Circ. Res. 88, 84e–87e.